



CROSSMARK

Journal of Taibah University for Science 11 (2017) 173–185

www.elsevier.com/locate/jtusci

Process optimization for the application of carbon from plantain peels in dye abstraction

E. Inam^{a,*}, U.J. Etim^b, E.G. Akpabio^a, S.A. Umoren^a

^a Department of Chemistry, Faculty of Science, University of Uyo, P.M.B. 1017, Uyo, Nigeria

^b School of Science, State Key Laboratory of Heavy Oil processing, China University of Petroleum, Huadong, 266280 Qingdao, PR China

Received 24 February 2015; received in revised form 7 January 2016; accepted 20 January 2016

Available online 4 March 2016

Abstract

Activated carbon obtained from plantain peels was applied to the optimization of the adsorption process parameters for abstraction of colour from simulated dye effluent. The activated carbon was prepared and characterized using nitrogen adsorption, X-ray diffractometry (XRD) and Fourier transform infrared spectroscopy (FTIR). Equilibrium isotherms were modelled using the Langmuir, Freundlich, Dubinin–Radushkevich and Temkin models; the Temkin and Dubinin–Radushkevich models provided the best fit for the sorption process, with a correlation coefficient greater than 0.95. The D–R model suggested a chemical process. The pseudo second-order kinetic model agreed well for fitting experimental data with the calculated adsorption capacity, q_e , (46.5 mg/g), which was reasonably close to the experimental value (47.3 mg/g). Optimization of the process parameters was achieved using response surface methodology (RSM) – Box–Behnken design, where factors considered are represented on three levels: (–1), (0) and (+1) for high, mean and low levels, respectively. ANOVA fits a quadratic model with prob > F less than 0.05 (<0.0001) at 95% confidence level. From this modelling, significant factors for dye removal have been identified.

© 2016 The Authors. Production and hosting by Elsevier B.V. on behalf of Taibah University. This is an open access article under the CC BY-NC-ND license (<http://creativecommons.org/licenses/by-nc-nd/4.0/>).

Keywords: Plantain peels; Activated carbon; Methylene blue; Adsorption; Process optimization

1. Introduction

Activated carbon has numerous applications, including liquid phase applications, gas phase applications, reduction of industrial air pollution and electrodes and

batteries. In liquid phase applications, activated carbon is used to treat industrial wastewaters, e.g., textile manufacturing wastewater. Activated carbon's large porous surface area and controllable pore structure make this material suitable for wastewater treatment [1]. The porosity of activated carbon facilitates the uptake of dyes; in this application, the chemical properties of dye and activated carbon are crucial due to the interactions that occur between the adsorbate and adsorbent [2,3]. Dye contamination of wastewater is a serious issue that affects dye and pigment-related industries [4,5]. Even at very low concentrations, dyes reduce general water quality by impairing important characteristics such as the

* Corresponding author. Tel.: +234 8181750861.

E-mail address: eduinam@uniuyo.edu.ng (E. Inam).

Peer review under responsibility of Taibah University.



Production and hosting by Elsevier

<http://dx.doi.org/10.1016/j.jtusci.2016.01.003>

1658–3655 © 2016 The Authors. Production and hosting by Elsevier B.V. on behalf of Taibah University. This is an open access article under the CC BY-NC-ND license (<http://creativecommons.org/licenses/by-nc-nd/4.0/>).

oxygen solubility level. The complex molecular structure of dyes makes them stable and difficult to biodegrade [6]. Methylene blue (MB), known for its wide application in textile industries, has harmful effects on living organisms during short periods of exposure [7]. In view of the above, plantain peels, a biowaste discarded in large quantities in most parts of the world, including Nigeria, can be used for the preparation of activated carbon [8]. Activated carbon prepared from plantain peels was utilized in the present study for dye abstraction from simulated dye wastewater. Plantain is a tropical crop from the genus *Musa* and is used as a food in many parts of the globe. Plantain peels are the outer layer of the plantain fruit, which is normally discarded as waste during food preparation. Many methods for removing dye from effluents have been studied [9]. Adsorption removes dyes with high efficiency. Carbon adsorbents made from biowaste, which consists primarily of cellulosic matter, exhibit high efficiency in removing dyes. Activated carbon produced from agricultural waste is effective for the adsorption of dyes from solution [10–14] because of its high surface area, as well as its micropore and mesopore structures. The micro- and mesopores develop during activation at high temperature. Few studies have been published employing plantain peels to produce activated carbon. Opeoyu and Fatoki [15] studied the dynamics of adsorption of zinc from an aqueous matrix using plantain peels. The adsorption efficiency of the biomass was greater than 99% for Zn^{2+} . Idowo et al. [16] studied the biosorption of chromium (VI) from aqueous solution using the biomass of plantain peel residue; the biomass was suitable for certain applications. Akpor et al. [17] used plantain peels in the removal of phosphorus and nitrogen from aqueous solution. The authors suggested the use of plantain peels for the bioremediation of wastewater. In a study by Adeyi et al. [12], carbon from plantain peels was used successfully to clean up effluent contaminated with aniline blue from textile industries. The adsorption of dyes has been studied with several sorbents using mathematical models, e.g., response surface. These studies are important for understanding the process and optimizing conditions for high adsorption [18–20].

Response surface methodology (RSM) is a set of mathematical techniques that describes the relationship among several independent variables and one or more dependent variables (responses). This method was developed by Box and Wilson [21] and has been widely used as a technique for designing experiments. This technique is useful in the fields of science and engineering, especially for better understanding and improving the efficiency of a process. RSM varies all significant

parameters simultaneously over a set of designed experiments and then combines the results through a mathematical model [22,23]. Box and Behnken [24] developed a model that accurately describes linear, quadratic and interaction effects of a second-order polynomial. This design was created to minimize the number of experiments in quadratic model fitting. Experimental matrices are constructed while taking into account two levels: high (+1) and low (−1) levels. The final matrix is completed by introducing a medium level and several replications of the central point, which reduces error.

In this paper, we employed Box–Behnken design (BBD) to optimize the adsorption process parameters for the adsorption of methylene blue (MB) from simulated dye effluent using activated carbon prepared from plantain peels; MB is a representative dye commonly used in the textile industry. The interactive effects of the process parameters were studied using this model. Kinetic and equilibrium studies were analysed to assess the validity of the statistical model and to determine the type of adsorption process.

2. Experimental

All chemical reagents, including H_2SO_4 , NaOH, HCl and MB (Fig. 1), were of analytical grade and were used as received. Plantain peels were collected from a disposal outlet in Uyo Metropolis, Nigeria. Details for preparation methods have been published elsewhere [8]. The prepared activated carbons (PAPP) and (CAPP), along with the nonactivated sample (NAPP), were characterized for surface area, porosity, surface functional groups and crystalline structure. The surface area and porosity analyses were carried out using a Micromeritics Surface area and porosity Analyser (Model: TriStar 3000) by nitrogen adsorption method at -196°C after pretreatment at 300°C for 4 h. The surface areas and pore volumes were determined online with the analyser program. The surface functional groups were detected by FTIR

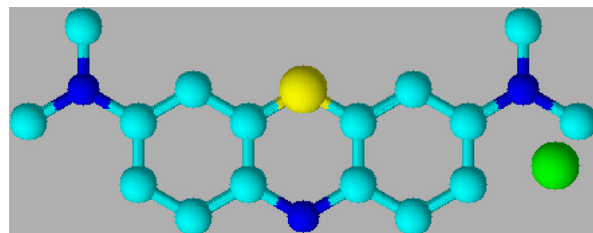


Fig. 1. 3D-molecular ball and stick structure of methylene blue: colour code; blue – nitrogen, orange – sulphur, green – chlorine and light blue – CH.

Table 1
Process variables and levels.

Factors	Levels		
	Low (−1)	Mean (0)	High (+1)
Initial dye concentration (mg/dm ³) (X_1)	50	175	300
Adsorbent weight (mg) (X_2)	100	350	600
Contact time (min) (X_3)	2	16	30

Table 2
Experimental design matrix for optimization using BBD.

Runs	Initial concentration (X_1)	Adsorbent weight (X_2)	Contact time (X_3)	Predicted value
1	−1	−1	0	22.39
2	+1	−1	0	46.46
3	−1	+1	0	16.04
4	+1	+1	0	40.41
5	−1	0	−1	15.90
6	+1	0	−1	40.12
7	−1	0	+1	17.68
8	+1	0	+1	41.90
9	0	−1	−1	30.71
10	0	+1	−1	27.76
11	0	−1	+1	35.74
12	0	+1	+1	26.29
13	0	0	0	28.70

spectrophotometry (Nicolet 6700, USA). XRD of the samples was analysed with a powder X-ray (Shimadzu XRD-6000) diffractometer using Cu K α radiation at a scanning rate of 6°/min, with 2θ ranging from 5° to 60°.

2.1. Design of experiment

Batch adsorption was employed in an optimization study of the following three independent parameters: initial dye concentration (X_1), adsorbent weight (X_2), and contact time (X_3) (Table 1). The optimization study followed carefully designed experiments using expert design (Version 7.0) with a BBD of the RSM. In total, 17 experiments with all possible combinations of parameters were run in duplicate. The average adsorption capacity, $q_{e,av}$ (mg/g) was used to obtain predicted responses (Table 2) according to their low, medium and high levels represented by −1, 0 and +1, respectively. The number of experiments was calculated according to Eq. (1),

$$N = k^2 + k + r, \quad (1)$$

where N is the total number of experiments, k is the number of studied factors and r is the replicate number of central points [5].

2.2. Preparation of adsorbate and adsorption process

A stock solution of 1 g/dm³ MB was prepared by dissolving 0.5 g of the dye in distilled water in a 0.5-dm³ volumetric flask and filling the flask to the mark. Working solutions were prepared from this stock solution by serial dilution to the desired concentrations; these solutions were used to generate a calibration curve (Fig. 2).

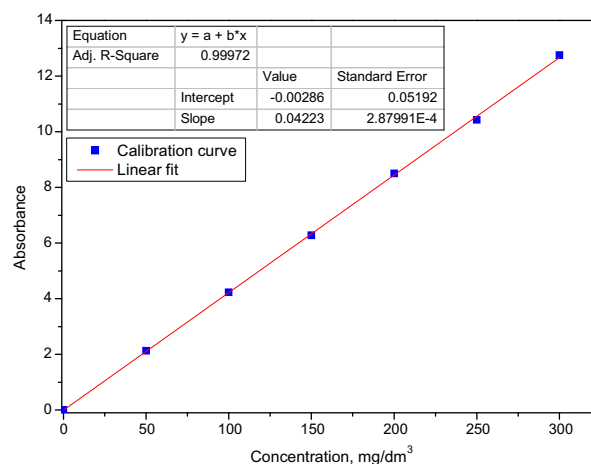


Fig. 2. Calibration curve for methylene blue absorption.

The adsorptive application of the prepared carbons was evaluated using a batch process and wastewater produced from a simulated dyeing process. Arbitrary concentrations (150 mg adsorbent weight and 200 mg/dm³ dye solution) were selected to evaluate the prepared adsorbents. Percentage adsorption, R , was calculated using Eq. (2).

$$R(\%) = \frac{C_i - C_f}{C_i} \times 100 \quad (2)$$

where C_i is the concentration of dye before adsorbent addition and C_f is the concentration of dye remaining in solution at equilibrium. Experiments were carried out to study the factors for maximum adsorption; the details are shown in Tables 1 and 2. The initial dye concentration, adsorbent weight and contact time were varied on three levels according to Table 2. pH was maintained at 3.0 throughout the experiment. This pH was chosen based on literature reports that found this pH maximized adsorption due to the existence of negatively charged species on the surface of agricultural waste carbon [8,25]. The pH was adjusted using 0.1 M NaOH or HCl. The kinetics of the process was studied by adsorbing the dye at different time intervals ranging from 2 to 35 min. Then, 100 mg of the adsorbent was added to a 250 cm³ conical flask containing 30 cm³ of a 100 mg/dm³ dye solution. The mixture was stirred with a magnetic stirrer vibrating at 200 rpm at room temperature (300 ± 2 K) until equilibrium was reached. The isotherm study was conducted by varying the initial concentration of the dye from 50 to 300 mg/dm³ at a constant adsorbent weight of 100 mg/dm³. The batch was agitated for 30 min with a magnetic stirrer at constant temperature (300 ± 2 K). In each

experiment, the residual dye concentration was determined using a UV-spectrophotometer (Unicam Heλ, Model 2100) at a predetermined maximum wavelength of MB ($\lambda_{\max} = 665$ nm). The quantity of dye adsorbed at equilibrium (q_e , mg/g) was calculated according to Eq. (3).

$$q_e = \frac{V}{m}(C_i - C_f) \quad (3)$$

3. Results and discussion

3.1. Characterization of activated carbon

Characterization of the activated carbon's surface area and porosity, surface functional groups and crystalline structure was carried out using BET adsorption method, FTIR and XRD, respectively. The surface area and porosity results have been published elsewhere [8]. Both PAPP and CAPP exhibited greater surface area and mesoporosity compared with NAPP; this is due to a burn off of the volatile substances on the carbon's surface during activation [1,11,26]. CAPP had an S_{BET} of 297 m²/g, higher than PAPP and NAPP, which had S_{BET} values of 177 m²/g and 1.71 m²/g, respectively. These differences were due to cumulative chemical and heat activation; the changes in the surface areas were attributable to the pores in PAPP. The pores were created in PAPP through a release of organic volatiles and CO from fixed carbon, which is attributed to the larger pore size (meso/macropores) and usually contributes to lower surface area [1]. Pores with diameters <2 nm, 2–50 nm and >50 nm are classified as micropores, mesopores and macropores, respectively. Fig. 3a and b shows that most adsorption of gas molecules

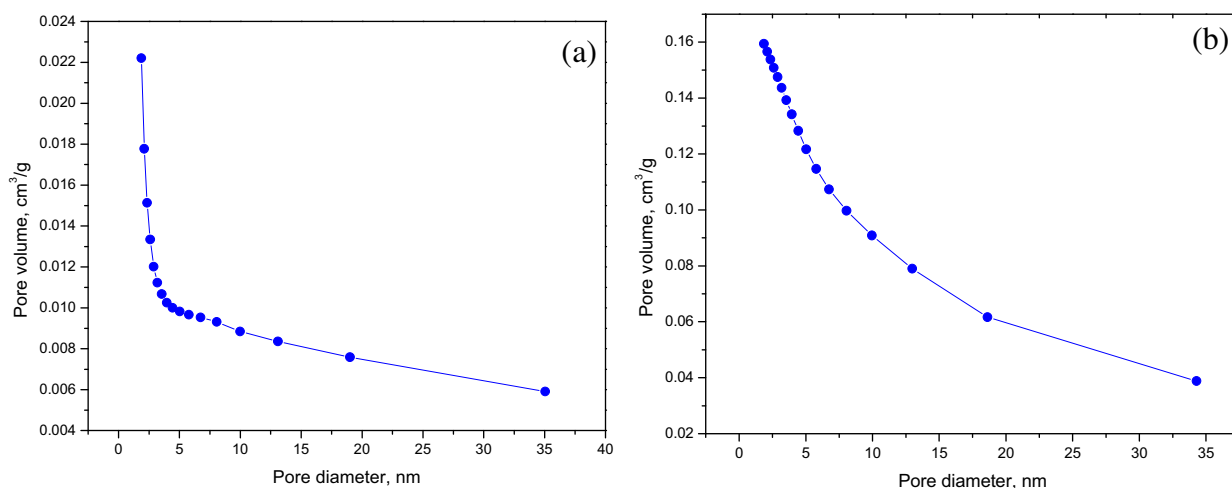


Fig. 3. Barrett, Joyner and Halenda (BJH) cumulative pore volume adsorption plot for activated carbon: (a) CAPP and (b) PAPP.

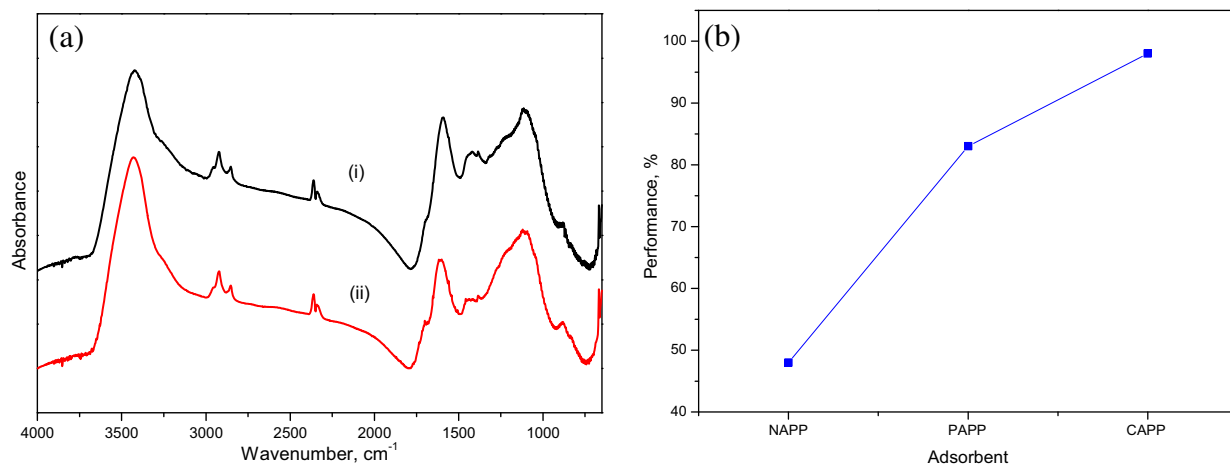


Fig. 4. (a) FTIR spectra of (i) CAPP, (ii) dye sorped CAPP and (b) adsorption evaluation for prepared activated carbons.

occurred on the low mesopores of the carbons; the mesopores had diameters of 1.8–5.0 nm and 1.8–3.5 nm for CAPP and PAPP, respectively. These observations indicate that the carbons were suitable for adsorption. Methylene blue has been reported to be successfully adsorbed onto mesopores with pore diameters greater than 1.5 nm [27–30].

In addition to the surface area and porosity, the performance of activated carbon is also influenced by surface chemistry. The different heteroatoms on the surface of activated carbon govern its chemistry. Heteroatoms such as oxygen, nitrogen and hydrogen are borne to peripheral carbon atoms and exist as organic functional groups [31]. The surface functional groups were studied using an FTIR spectrophotometer in the wave number range of 4000–400 cm^{-1} . The spectra [8] and Fig. 4a reveal different functional groups on the surface of PAPP, CAPP and NAPP of the plantain peels. The NAPP exhibits many heteroatoms, as revealed by the spectrum. The activation processes produce activated carbon and decreased the heteroatoms. The decrease in heteroatoms resulted in a decrease in vibration bands, as evidenced by the reduced intensity of certain peaks and the disappearance of some bands. This indicates that the activation processes for the production of PAPP and CAPP were efficient and led to oxidation of the functional groups of the starting material [32]. However, Fig. 4a shows spectra of the carbon surface before and after adsorption. The intensity of the vibration near 1425 cm^{-1} decreased. This is indicative of an interaction between the functional group on the surface of the carbon and a functional group from the dye [33].

3.2. Evaluation of activated carbons

The prepared activated carbons, PAPP and CAPP, were tested for their ability to effectively adsorb dyes compared with the NAPP (Fig. 4b). Abstraction of colour was in the order $\text{NAPP} < \text{PAPP} < \text{CAPP}$. Compared with NAPP, PAPP and CAPP were 35% and 50% more efficient, respectively. This might be related to the increase in surface area and pore volume, which invariably increased the micro-mesoporosity:macroporosity ratio in the structure of the carbons. In the PAPP, only approximately 6% pore volume is microporous; the rest are a combination of mesopores and macropores. The attribution of macroporosity to decreased surface area is documented in the literature [1]. Based on this evaluation, optimization, kinetics and isotherm studies were conducted with CAPP.

3.3. Equilibrium adsorption isotherm

Adsorption isotherms are invaluable tools for evaluating the performance of the adsorption process, describing how the adsorbent interacts with the adsorbate. Useful conclusions can be drawn for a process by relating the equilibrium concentration of a dye solution with adsorption capacity. Although several adsorption isotherms are known, only four important isotherms are analysed in the present report. The Langmuir isotherm [34], which describes monolayer attachment of gas or liquid molecules to the surface of an adsorbent, was applied according to Eq. (4). A plot of $1/q_e$ against $1/c_e$ (not shown) should be a straight line with a good correlation coefficient (R^2) to be reliable. b and q_o (Table 3)

Table 3
Equilibrium adsorption isotherm parameters.

Isotherms	Parameters		
Langmuir	b (dm ³ /mg)	q_o (mg/g)	R^2
	0.7489	19.044	0.8571
Freundlich	K_F (mg/g)(dm ³ /g) ^{1/n}	n	R^2
	3.4186	0.7164	0.9786
Temkin	b (J/mol)	K_T (dm ³ /g)	R^2
	5321.5	1.0221	0.9999
D–R	Q_m (mg/g)	K_E (mol ² /kJ ²)	R^2
	4.783	-5.68×10^{-6}	0.9649

are obtained from the slope and intercept of the plot, respectively. q_e (mg/g), c_e (mg/dm³), b (dm³/mg) and q_o (mg/g) are adsorption capacity, dye concentration at equilibrium, Langmuir isotherm constant and maximum adsorption capacity, respectively. The characteristic

nonlinear plot and poor R^2 value for this study made it insufficient to explain the adsorption process.

The Freundlich isotherm has been applied to study the heterogeneity of systems, especially for organic compounds or highly interactive species on activated carbon and molecular sieves [35]. Its linear form is represented by Eq. (5). A plot of $\log q_e$ against $\log C_e$ (Fig. 5a) gives a linear curve where constant K_F (Freundlich isotherm constant [(mg/g)(dm³/g)^{1/n}]) is related to adsorption capacity. K_F and n (adsorption intensity) are calculated from the intercept and slope of the plot, respectively. The slope ranging between 0 and 1 is a measure of adsorption intensity or surface heterogeneity; it becomes more heterogeneous as its value gets closer to zero [35]. In this study, $1/n$ is greater than unity, indicating cooperative adsorption.

The Temkin isotherm model provides useful insight into the adsorption mechanism as it explicitly accounts

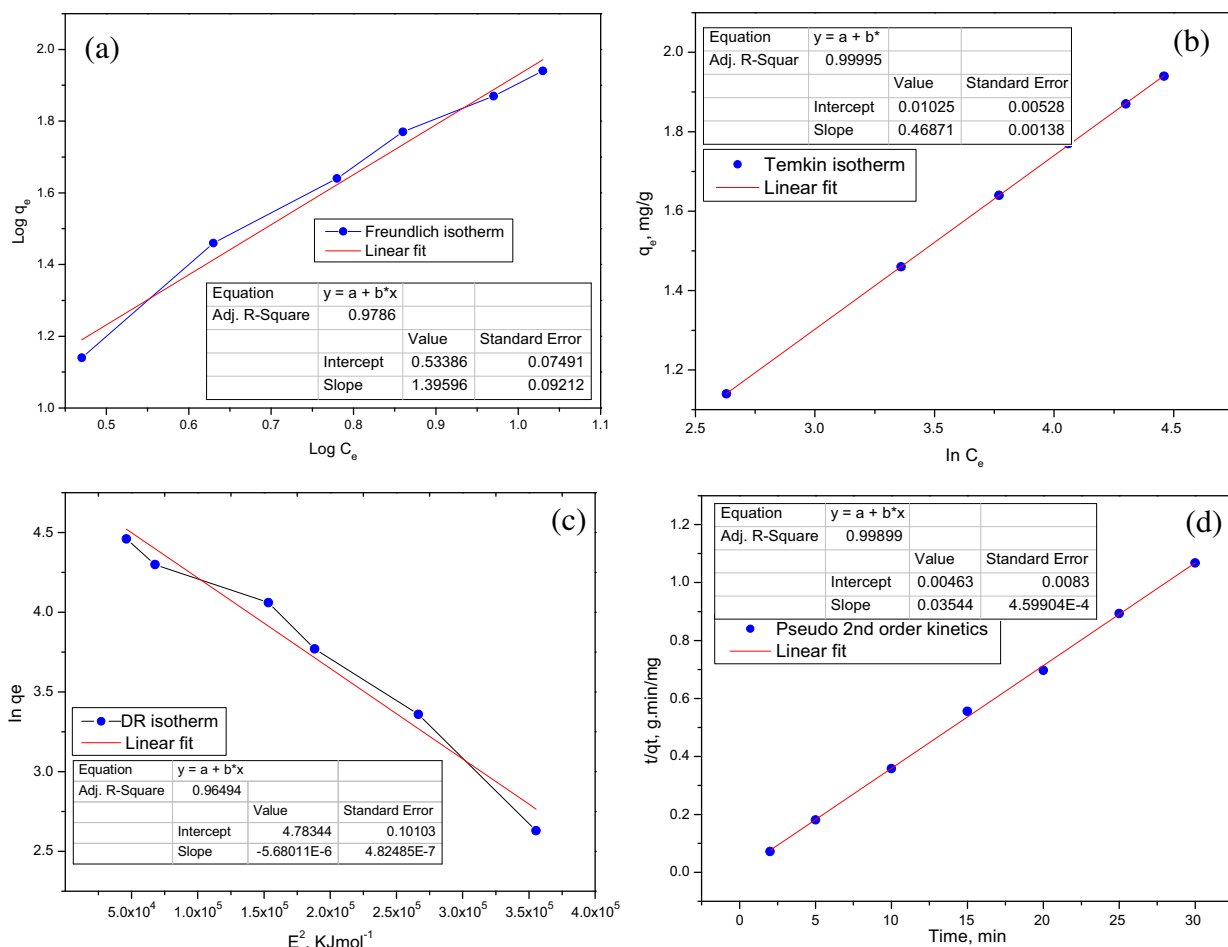


Fig. 5. (a) Freundlich isotherm plot. (b) Temkin isotherm plot. (c) Dubinin–Radushkevich plot. (d) Pseudo second-order kinetics plot for MB adsorption.

for adsorbent–adsorbate interactions and the energy of adsorption. This model assumes the heat of adsorption of all of the molecules in the layer decreases linearly with coverage due to adsorbent–adsorbate interactions. The adsorption is characterized by a uniform distribution of binding energies, up to some maximum binding energy [36]. The derivation of the Temkin isotherm assumes that the decrease in the heat of sorption is linear rather than logarithmic, as implied by the Freundlich equation [25]. The Temkin isotherm can be applied in the form given in Eq. (6), where T is the absolute temperature (K), R is molar gas constant (J/mol K), and K_T (dm³/g) and b (J/mol) are Temkin isotherm constants. By plotting q_e against $\ln C_e$ (Fig. 5b), K_T and b can be calculated from the intercept and slope of the straight line. Values of b and K_T (Table 3), 5321.5 J/mol and 1.0221 dm³/g, respectively, are within the validity frame of model fit for explaining this adsorption process. The process was endothermic as indicated with a positive energy value. The D–R isotherm was also used to estimate the apparent free energy of adsorption and type of adsorption [37]. The D–R equation can be written in the form of Eq. (7a), where K_E is a constant related to the adsorption energy (mol²/kJ²) and Q is, the theoretical D–R constant (mg/g). ε is the Polanyi potential and is calculated from Eq. (7b), where R is the molar gas constant (J/mol K) and T is absolute temperature (K). The values of Q_m and K_E were obtained from the intercept and slope, respectively, of the linear plot of $\ln q_e$ against ε^2 (Table 3). The mean adsorption energy, E (kJ/mol), can be obtained by applying the value of K_E of the D–R isotherm equation in Eq. (7c). Calculation gives a value of 296.7 kJ/mol for E . It has been documented that “ E ” provides useful information on the type/mechanism of adsorption process. If “ E ” is less than 8 kJ/mol, the adsorption is physical in nature; if it is between 8 and 16 kJ/mol, the adsorption process proceeds via ion exchange. If “ E ” is greater than 16 kJ/mol, the mechanism of particle diffusion and chemical reaction dominate the process [38–40]. Therefore, from this result, it is concluded that the process is chemisorption.

$$\frac{1}{q_e} = \frac{1}{q_o} + \frac{1}{bC_e q_o} \quad (4)$$

$$\log q_e = \log K_F + \frac{1}{n} \log C_e \quad (5)$$

$$q_e = \frac{RT}{b} \ln K_T + \frac{RT}{b} \ln C_e \quad (6)$$

$$\ln q_e = \ln Q_m - K_E \varepsilon^2 \quad (7a)$$

$$\varepsilon = RT \ln \left[1 + \frac{1}{C_e} \right] \quad (7b)$$

$$E = (-2K_E)^{-1/2} \quad (7c)$$

3.4. Adsorption kinetics

Adsorption kinetics was studied to understand the dynamics of the system, applying pseudo-first and pseudo-second-order models. The linear form of pseudo-first-order dynamics is given by Eq. (8). A plot of $\log(q_e - q_t)$ against t (not shown) is expected to be linear for applicability of the model. However, for this study, the data deviated largely from linearity and was inapplicable. In Eq. (8), q_e is the adsorption capacity at equilibrium (mg/g), q_t is instantaneous adsorption capacity (mg/g), t is time (min) and K_1 (/min) is the rate constant for the reaction order. K_1 and q_e are 0.231/min and 21.8 mg/g, respectively, with $R^2 < 0.7$. These values are typical of a nonconforming model for this work. Experimental data fit a pseudo-second-order kinetic model with a good correlation coefficient, $R^2 = 0.9989$; q_e (46.8 mg/g) approaches an experimental value of 47.3 mg/g. Parameters evaluating the applicability of pseudo second order reaction were obtained from the plot of t/q_t against t (Fig. 5d) in Eq. (9), where K_2 is the rate constant for the reaction and the other terms have their usual meanings. The fitting of a pseudo-second-order kinetic model confirms the earlier proposition from the D–R isotherm that the process is a chemisorption process.

$$\text{Log}(q_e - q_t) = \text{Log } q_e - \frac{K_1}{2.303} t \quad (8)$$

$$\frac{t}{q_t} = \frac{1}{K_2 q_e^2} + \frac{1}{q_e} t \quad (9)$$

3.5. Statistical analysis of regression model

Experiment design provides a statistical model that uses quantitative data to determine regression model equations for the optimization of operating conditions [41]. The Box–Behnken design of RSM was employed to optimize conditions for maximum adsorption of MB on carbon from plantain peels. The methodology is practical because it employs experimental data and explores the interactive effects of the variables on the overall process. Statistical analysis was carried out by fitting experimental data to a general model equation given in Eq. (10) [42],

$$Y = \beta_o + \sum_{j=1}^k \beta_j x_j + \sum_{j=1}^k \beta_{jj} x_j^2 + \sum_{i>j} \beta_{ij} x_i x_j + e_i \quad (10)$$

Table 4
ANOVA for response surface quadratic model.

Source	Sum of squares	Degree of freedom	Mean square	F-value	Prob > F	
Model	1286.31	9	142.9	85.16	<0.0001	Significant
X_1	1173.7	1	1174	699.4	<0.0001	Significant
X_2	76.88	1	76.88	45.81	0.0003	Significant
X_3	6.3	1	6.3	3.75	0.0939	
X_1X_2	0.023	1	0.023	0.013	0.9111	
X_1X_3	0	1	0	0	1	
X_2X_3	10.56	1	10.56	6.29	0.0405	
X_1^2	2.06	1	2.06	1.23	0.3042	
X_2^2	15.6	1	15.6	9.3	0.0186	
X_3^2	1.05	1	1.05	0.63	0.4544	
Residual	11.75	7	1.68			
Lack of fit	11.75	3	3.92			
Pure error	0	4	0			

where Y is the response; β_o is a constant coefficient; β_j , β_{jj} and β_{ij} are interaction coefficients of linear, quadratic and second-order terms, respectively; x_i and x_j are the independent variables; k is the number of studied factors; and e_i is the error term. The coded values of the process parameters in Eq. (10) could be determined by Eq. (11) where x_i is the dimensionless coded value of the i th independent variable, x_i is the uncoded value of the i th independent variable, x_o is the uncoded value of the i th independent variable at the centre point and Δx_i is the step change value between low level (-1) and high level ($+1$) [43].

$$X_i = \frac{x_i - x_o}{\Delta x_i} \quad (11)$$

The transformed model equation in terms of coded factors is given in Eq. (12).

$$\begin{aligned} q_e = & 28.7 + 12.11X_1 - 3.10X_2 + 0.89X_3 \\ & + 0.075X_1X_2 - 1.63X_2X_3 + 0.70X_1^2 \\ & + 1.92X_2^2 - 0.50X_3^2, \end{aligned} \quad (12)$$

where q_e is the predicted adsorption capacity. Eq. (12) can be used to make predictions about the response in terms of coded factors for a given level of each factor. The high and low levels for the factors are coded as $+1$ and -1 , respectively. The relative impact of the factors is determined by comparing the factor's coefficients. The initial concentration is indicated by

the coefficient to have a significant impact on adsorption. The significance of the model equation and the goodness of fit were evaluated by the F -test analysis of variance (ANOVA) (Table 4) and R^2 values (Table 5). The ANOVA subdivides the total variation in a set of data into components associated with specific sources of variation to test hypotheses on the parameters of the model [44]. It also identifies important factors and determines which is the most significant and if the experiment results are meaningful. A large F -value indicates that most of the variation can be explained by a regression equation and a low p -value (<0.05) points to a statistically significant model. The responses (see Table 2) were calculated according to Eq. (12), and the data were verified by the coefficients of each of the terms in Table 4. The significance of each coefficient was measured from the probability values (p -values). The model F -value (85.16) implies that the model is significant. Values of $P(F > 0.1)$ indicate that the model terms are not significant. In this process, X_1 and X_2 , are the most significant terms (Table 4). Good values that predict an accurate response for the standard deviation, coefficient of variation, adjusted R^2 and predicted R^2 are 0.92, 3.11, 0.9853 and 0.8558, respectively (Table 5). Generally, the coefficient of variation (CV), which is the ratio of the standard error to the mean value of the observed response measures reproducibility of the model. A model can be considered reasonable if its CV is less than 15% [45].

Table 5
Model fit summary for quadratic model1.

Model statistics						
Std. dev.	Mean	CV (%)	Press	R^2	Adj R^2	Pred. R^2
0.92	29.41	3.11	187.96	0.9910	0.9852	0.8558

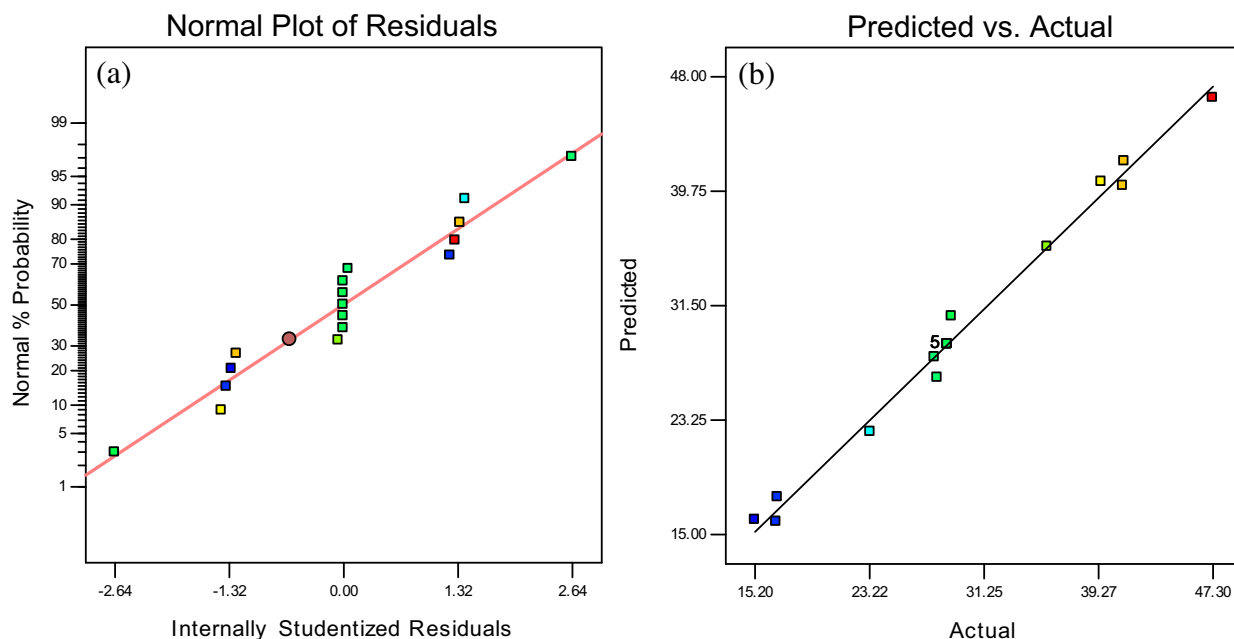


Fig. 6. (a) Normal probability plot of studentized individuals and (b) predicted against actual values of adsorption capacity for MB adsorption.

Although predicted R^2 is less than adjusted R^2 , it is considered to be in reasonable agreement if the difference is less than 0.2 threshold value. The R^2 value (0.991) is indicative of the model providing 99.1% accuracy of output prediction. Cobas et al. [5] and Isa et al. [42] recorded model outputs of approximately 95.3% and 97%, respectively, indicated nonbias models. The validity of the model was confirmed by the diagnostic plots; normal probability plots of studentized residuals and plots of predicted values against actual values (Fig. 6). While the former shows a good distribution of data at experimental points, the latter shows that predicted and actual values agree well. These results indicate that the statistical analysis data confirms the experimental data to a significant degree of certainty.

3.6. Effect of variables interaction on adsorption

Fig. 7 shows the effect of the interaction of any two factors in the adsorption process while the other factor remained constant. The simultaneous effect of time and initial concentration is presented (Fig. 7a). The adsorption capacity increases with an increase in concentration. This means that at a higher concentration, there is a greater driving force to overcome mass transfer limitations, leading to higher adsorption. From the figure, adsorptive removal was exclusively concentration dependent as revealed by the intense contour gradient

at high concentrations. The interactive effect of adsorbent weight and initial concentration is shown in Fig. 7b. Obviously, the two factors have an overwhelming influence on the response. The gradient of the contour tilts the lower right corner of the plot, implying a high performance at high concentration and low adsorbent weight. Although increases in adsorbent weight increase the adsorption, in this study, adsorption sites corresponding to 100 mg showed maximum adsorption. In Fig. 7c, the effect of time and adsorbent is shown; the adsorbent weight is the limiting factor even at very short contact times. The interactive effects of these variables demonstrate the impact of each factor on the response. Nevertheless, the most important factor controlling the response can also be shown with the perturbation plot (Fig. 7d). The response is plotted by changing only one factor over its range while holding the other factors constant. The perturbation plot compares the effect of all of the factors at a particular point in the design space. As seen from the plot, concentration is the most significant factor for this process, which varies greatly with adsorption capacity.

3.7. Process optimization

Process optimization was achieved using the numerical node of the design expert software. The three studied variables were targeted within the range (high and low) and the adsorption capacity (response) was targeted at

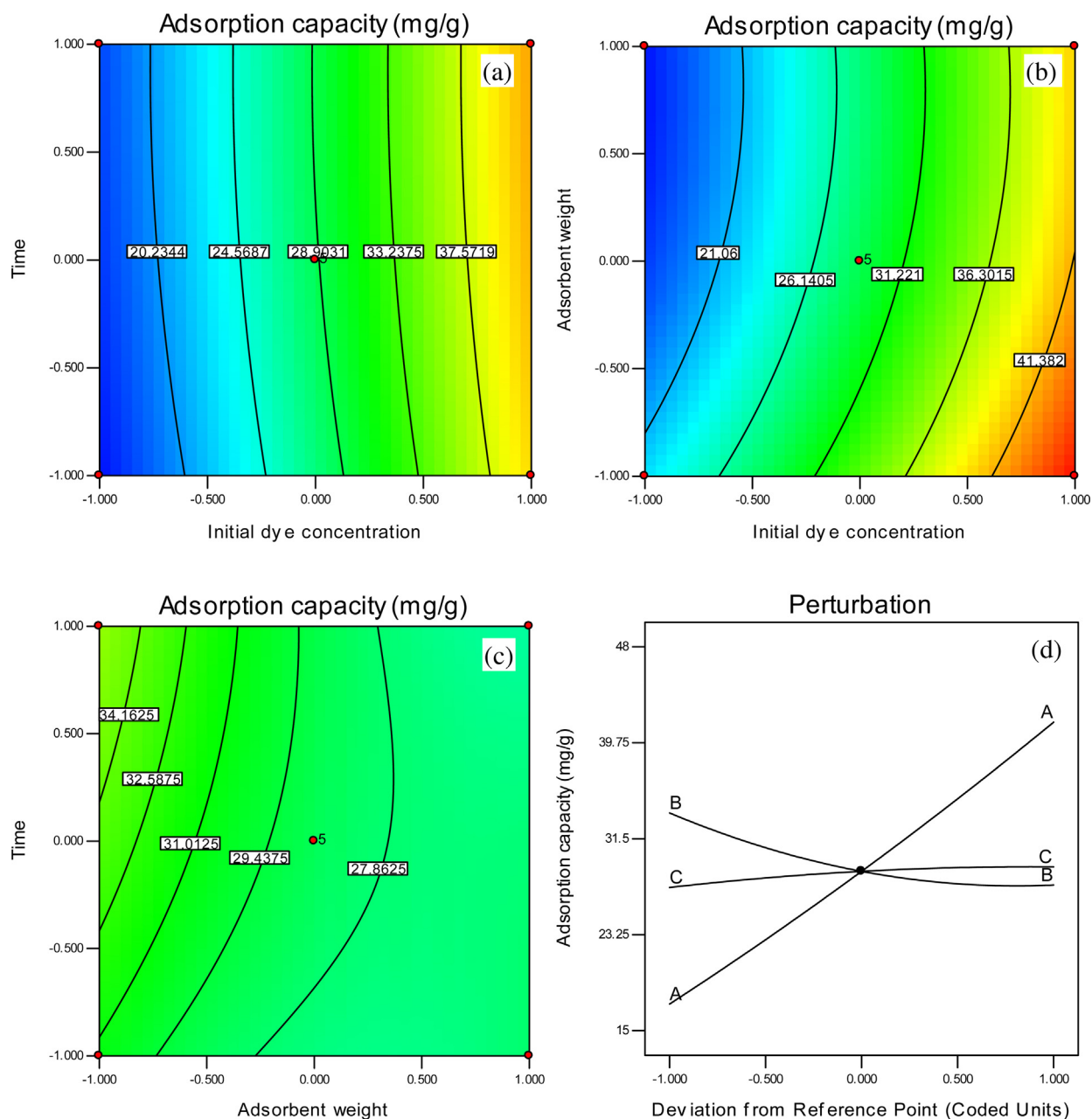


Fig. 7. Contour plot showing effect on adsorption capacity of combined factors (a) time and initial concentration, (b) adsorbent weight and initial concentration, (c) time and adsorbent weight and (d) perturbation plot showing effect of individual factors at the medium level.

the maximum. The program integrates individual factors at tuneable levels and output response (Fig. 8a–e). Variation of the factors produces an important result which leads to optimal conditions. Notably, time was not a crucial factor for this experiment; a time of 5 min was enough to obtain a 44.2 mg/g adsorption performance (Fig. 8). When the factors were varied between extreme conditions an optimal response of 48.4 mg/g

was obtained as seen in the cube plot (Fig. 9); the extreme conditions include a concentration set at maximum (300 mg/dm^3), an adsorbent weight minimum (100 mg) and time of 30 min. The cube plot represents the effect of three factors simultaneously, showing the predicted values from the coded model for the combinations of the -1 and $+1$ levels of the three factors.

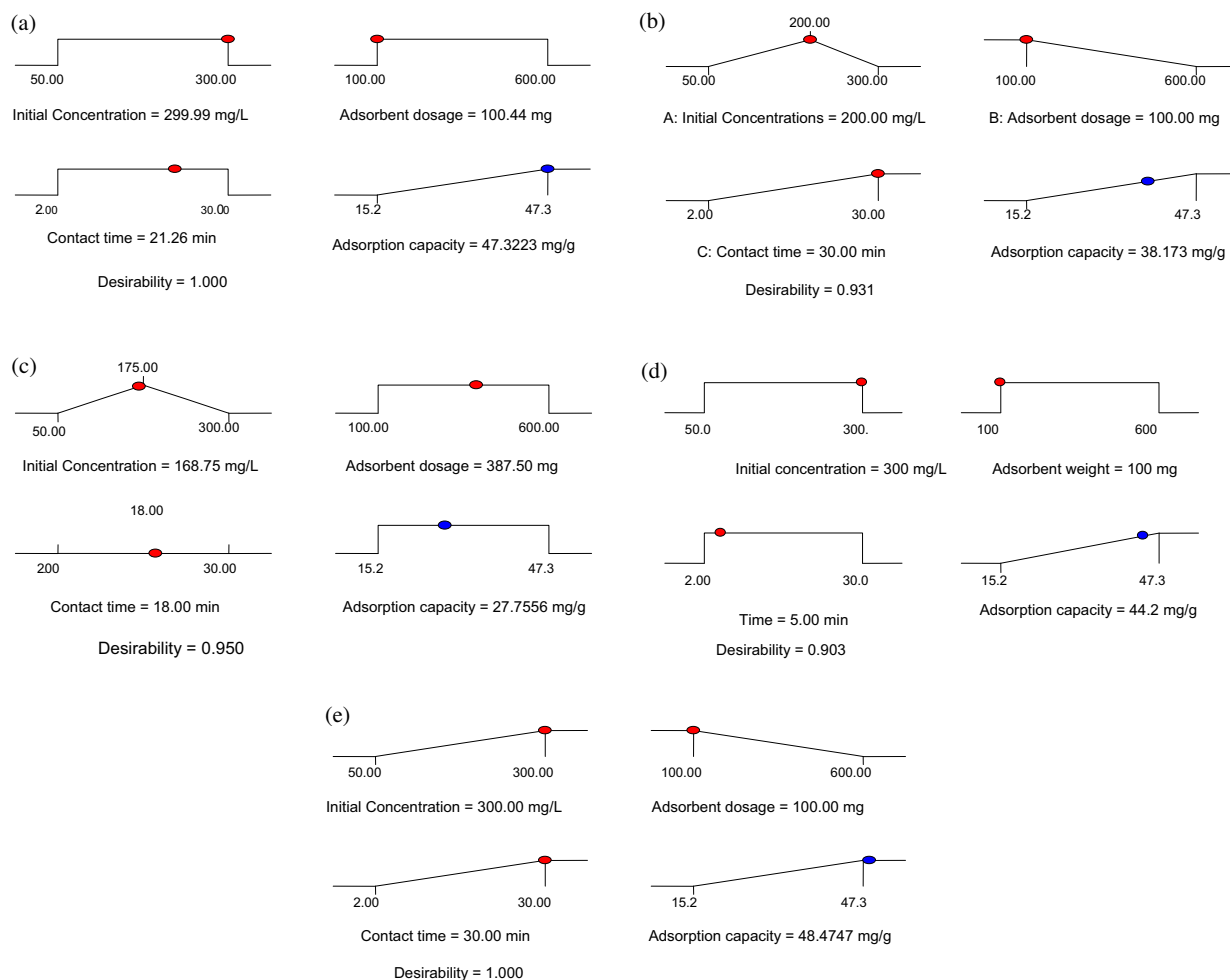


Fig. 8. Desirability ramp for numerical optimization for independent factors (initial concentration, adsorbent weight, time), and response (adsorption capacity).

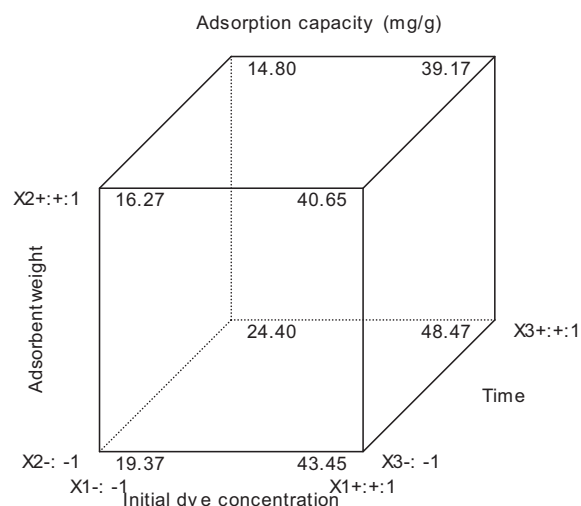


Fig. 9. Cube plot for surface response of MB adsorption onto plantain peels carbon.

4. Conclusion

Activated carbon prepared from plantain peels is suitable for MB adsorption from simulated dye wastewater. Its performance suggests that it is applicable to the treatment of industrial dye wastewater. The good adsorption capacity of the CAPP is closely related to its high S_{BET} and mesopore size distribution. FTIR analysis of the carbon surface revealed functional groups that are involved in adsorption through interactions with dye molecules. The mechanism of adsorption shown by FTIR, conformity of adsorption to Temkin and D-R isotherms, and pseudo-second-order kinetic models revealed an endothermic chemisorption process. With the help of Box–Behnken design of RSM, two factors, namely, initial dye concentration and adsorbent weights, are identified to significantly favour the adsorption process.

Acknowledgements

The authors thank members of Laboratory of Catalysis, State Key Laboratory of Heavy Oil processing, China University of petroleum for use of their facilities for adsorbent characterization.

References

- [1] M. Asadullah, M.S. Kabir, M.B. Ahmed, N.A. Razak, N.S.A. Rasid, A. Aezzira, Role of microporosity and surface functionality of activated carbon in methylene blue dye removal from water, *Korean J. Chem. Eng.* 30 (2013) 2228–2234.
- [2] B.S. Girgis, A.-N.A. El-Hendawy, Porosity development in activated carbons obtained from date pits under chemical activation with phosphoric acid, *Micropor. Mesopor. Mater.* 52 (2002) 105–117.
- [3] N. Karatepe, İ. Orbak, R. Yavuz, A. Özyüğür, Sulfur dioxide adsorption by activated carbons having different textural and chemical properties, *Fuel* 87 (2008) 3207–3215.
- [4] O.S. Bello, K.A. Adegoke, A.A. Olaniyan, H. Abdulazeez, Dye adsorption using biomass wastes and natural adsorbents: overview and future prospects, *Desalin. Water Treat.* 53 (2015) 1292–1315.
- [5] M. Cobas, M. Sanromán, M. Pazos, Box–Behnken methodology for Cr (VI) and leather dyes removal by an eco-friendly biosorbent: *F. vesiculosus*, *Bioresour. Technol.* 160 (2014) 166–174.
- [6] D. Podstawczyk, A. Witek-Krowiak, K. Chojnacka, Z. Sadowski, Biosorption of malachite green by eggshells: mechanism identification and process optimization, *Bioresour. Technol.* 160 (2014) 161–165.
- [7] G.O. El-Sayed, Removal of methylene blue and crystal violet from aqueous solutions by palm kernel fiber, *Desalination* 272 (2011) 225–232.
- [8] E.I. Inam, U.J. Etim, E.G. Akpabio, S.A. Umoren, Simultaneous adsorption of lead (II) and 3,7-bis (dimethylamino)-phenothiazin-5-ium chloride from aqueous solution by activated carbon prepared from plantain peels, *Desalin. Water Treat.* (2015) 1–14, <http://dx.doi.org/10.1080/19443994.2015.1010236>.
- [9] V. Gupta, Application of low-cost adsorbents for dye removal – a review, *J. Environ. Manage.* 90 (2009) 2313–2342.
- [10] M. Asadullah, M. Asaduzzaman, M.S. Kabir, M.G. Mostofa, T. Miyazawa, Chemical and structural evaluation of activated carbon prepared from jute sticks for Brilliant Green dye removal from aqueous solution, *J. Hazard. Mater.* 174 (2010) 437–443.
- [11] M. Asadullah, I. Jahan, M.B. Ahmed, P. Adawiyah, N.H. Malek, M.S. Rahman, Preparation of microporous activated carbon and its modification for arsenic removal from water, *J. Ind. Eng. Chem.* 20 (2014) 887–896.
- [12] O. Adeyi, O.S. Ayanda, G.O. Olutona, O. Ganiyu, Adsorption kinetics and intraparticle diffusivity of aniline blue dye onto activated plantain peels carbon, *Chem. Sci. Trans.* (2012).
- [13] J.M. Dias, M.C. Alvim-Ferraz, M.F. Almeida, J. Rivera-Utrilla, M. Sánchez-Polo, Waste materials for activated carbon preparation and its use in aqueous-phase treatment: a review, *J. Environ. Manage.* 85 (2007) 833–846.
- [14] A. Ahmad, M. Loh, J. Aziz, Preparation and characterization of activated carbon from oil palm wood and its evaluation on methylene blue adsorption, *Dyes Pigm.* 75 (2007) 263–272.
- [15] B. Opeolu, O. Fatoki, Dynamics of zinc sorption from aqueous matrices using plantain (*Musa* sp.) peel biomass, *Afr. J. Biotechnol.* 11 (2012) 13194–13201.
- [16] S. Idowu, S. Oni, A. Adejumo, Biosorption of chromium (VI) from aqueous solution by biomass of plantain (*Musa paradisiaca*) peel residue, *Afr. J. Med. Phys. Biomed. Eng. Sci.* 3 (2011) 22.
- [17] O. Akpor, C. Nwonuma, T. Edewor-Kuponiyi, O. Amira, The role of ripe *Musa sapientum* (plantain) peels in the removal of phosphorus and nitrogen from aqueous solution, *J. Biol. Agric. Health* 3 (2013) 85–96.
- [18] M. Ghaedi, S.N. Kokhdan, Removal of methylene blue from aqueous solution by wood millet carbon optimization using response surface methodology, *Spectrochim. Acta A* 136 (2015) 141–148.
- [19] S. Dutta, A. Bhattacharyya, A. Ganguly, S. Gupta, S. Basu, Application of response surface methodology for preparation of low-cost adsorbent from citrus fruit peel and for removal of methylene blue, *Desalination* 275 (2011) 26–36.
- [20] M.D. Pavlović, A.V. Buntić, K.R. Mihajlovski, S.S. Šiler-Marinković, D.G. Antonović, Ž. Radovanović, S.I. Dimitrijević-Branković, Rapid cationic dye adsorption on polyphenol-extracted coffee grounds—a response surface methodology approach, *J. Taiwan Inst. Chem. Eng.* 45 (2014) 1691–1699.
- [21] G.E. Box, K. Wilson, On the experimental attainment of optimum conditions, *J. R. Stat. Soc. Ser. B* 13 (1951) 1–45.
- [22] R.H. Myers, D.C. Montgomery, C.M. Anderson-Cook, *Response Surface Methodology: Process and Product Optimization Using Designed Experiments*, 3rd ed., John Wiley & Sons, New York, 2009.
- [23] F. Ghorbani, H. Younesi, S.M. Ghasempouri, A.A. Zinatizadeh, M. Amini, A. Daneshi, Application of response surface methodology for optimization of cadmium biosorption in an aqueous solution by *Saccharomyces cerevisiae*, *Chem. Eng. J.* 145 (2008) 267–275.
- [24] G.E. Box, D.W. Behnken, Some new three level designs for the study of quantitative variables, *Technometrics* 2 (1960) 455–475.
- [25] P.S. Kumar, S. Ramalingam, C. Senthamarai, M. Niranjana, P. Vijayalakshmi, S. Sivanesan, Adsorption of dye from aqueous solution by cashew nut shell: studies on equilibrium isotherm, kinetics and thermodynamics of interactions, *Desalination* 261 (2010) 52–60.
- [26] O. Olorundare, R. Krause, J. Okonkwo, B. Mamba, Potential application of activated carbon from maize tassel for the removal of heavy metals in water, *Phys. Chem. Earth* 50 (2012) 104–110.
- [27] Y. Gao, Q. Yue, B. Gao, Y. Sun, Optimization preparation of activated carbon from *Enteromorpha prolifera* using response surface methodology and its adsorption studies of fluoroquinolone antibiotics, *Desalin. Water Treat.* (2014) 1–13.
- [28] F. Ahmad, W.M.A.W. Daud, M.A. Ahmad, R. Radzi, Cocoa (*Theobroma cacao*) shell-based activated carbon by CO₂ activation in removing of cationic dye from aqueous solution: kinetics and equilibrium studies, *Chem. Eng. Res. Des.* 90 (2012) 1480–1490.
- [29] S. Altenor, B. Carene, E. Emmanuel, J. Lambert, J.-J. Ehrhardt, S. Gaspard, Adsorption studies of methylene blue and phenol onto vetiver roots activated carbon prepared by chemical activation, *J. Hazard. Mater.* 165 (2009) 1029–1039.
- [30] S. Wang, Z. Zhu, A. Coomes, F. Haghseresht, G. Lu, The physical and surface chemical characteristics of activated carbons and the adsorption of methylene blue from wastewater, *J. Colloid Interface Sci.* 284 (2005) 440–446.

- [31] Y. El-Sayed, T.J. Badosz, Adsorption of valeric acid from aqueous solution onto activated carbons: role of surface basic sites, *J. Colloid Interface Sci.* 273 (2004) 64–72.
- [32] N.F. Cardoso, R.B. Pinto, E.C. Lima, T. Calvete, C.V. Amavisca, B. Royer, M.L. Cunha, T.H. Fernandes, I.S. Pinto, Removal of remazol black B textile dye from aqueous solution by adsorption, *Desalination* 269 (2011) 92–103.
- [33] U.J. Etim, S. AUmoren, U.M. Eduok, Coconut coir dust as a low cost adsorbent for the removal of cationic dye from aqueous solution, *J. Saudi Chem. Soc.* (2012), <http://dx.doi.org/10.1016/j.jscs.2012.09.014>.
- [34] I. Langmuir, The constitution and fundamental properties of solids and liquids. Part I. Solids, *J. Am. Chem. Soc.* 38 (1916) 2221–2295.
- [35] K. Foo, B. Hameed, Insights into the modeling of adsorption isotherm systems, *Chem. Eng. J.* 156 (2010) 2–10.
- [36] M. Temkin, V. Pyzhev, Recent modifications to Langmuir isotherms, *Acta Physicochim. USSR* 12 (1940) 217–222.
- [37] M. Dubinin, L. Radushkevich, Equation of the characteristic curve of activated charcoal, *Chem. Zentr.* 1 (1947) 875.
- [38] X.-W. Wu, H.-W. Ma, Y.-R. Zhang, Adsorption of chromium (VI) from aqueous solution by a mesoporous aluminosilicate synthesized from microcline, *Appl. Clay Sci.* 48 (2010) 538–541.
- [39] M.E. Argun, S. Dursun, C. Ozdemir, M. Karatas, Heavy metal adsorption by modified oak sawdust: thermodynamics and kinetics, *J. Hazard. Mater.* 141 (2007) 77–85.
- [40] S. Tahir, N. Rauf, Removal of a cationic dye from aqueous solutions by adsorption onto bentonite clay, *Chemosphere* 63 (2006) 1842–1848.
- [41] A. Zahangir, S.A. Muyibi, J. Toramae, Statistical optimization of adsorption processes for removal of 2,4-dichlorophenol by activated carbon derived from oil palm empty fruit bunches, *J. Environ. Sci.* 19 (2007) 674–677.
- [42] M.H. Isa, E.H. Ezechi, Z. Ahmed, S.F. Magram, S.R.M. Kutty, Boron removal by electrocoagulation and recovery, *Water Res.* 51 (2014) 113–123.
- [43] H. Zhang, X. Ran, X. Wu, D. Zhang, Evaluation of electro-oxidation of biologically treated landfill leachate using response surface methodology, *J. Hazard. Mater.* 188 (2011) 261–268.
- [44] K. Ravikumar, K. Pakshirajan, T. Swaminathan, K. Balu, Optimization of batch process parameters using response surface methodology for dye removal by a novel adsorbent, *Chem. Eng. J.* 105 (2005) 131–138.
- [45] R.J. Rossi, *Applied Biostatistics for the Health Sciences*, John Wiley & Sons, New Jersey, 2010.